

Received 26 June 2017; revised 20 September 2017; accepted 22 September 2017.
Date of publication 29 September 2017; date of current version 12 October 2017.

Digital Object Identifier 10.1109/JTEHM.2017.2757485

Simultaneous Tracking of Cardiorespiratory Signals for Multiple Persons Using a Machine Vision System With Noise Artifact Removal

ALI AL-NAJI^{1,2}, (Member, IEEE), AND JAVAAN CHAHL^{1,3}, (Member, IEEE)

¹School of Engineering, University of South Australia, Mawson Lakes, SA 5095, Australia

²Electrical Engineering Technical College, Middle Technical University, Baghdad 10022, Iraq

³Joint and Operations Analysis Division, Defence Science and Technology Group, Melbourne, VIC 3207, Australia

CORRESPONDING AUTHOR: A. AL-NAJI (ali_abdulah_noori.al-naji@mymail.unisa.edu.au)

This work was supported by the Defence Science and Technology Group's Tyche Program on trusted autonomy.

ABSTRACT Most existing non-contact monitoring systems are limited to detecting physiological signs from a single subject at a time. Still, another challenge facing these systems is that they are prone to noise artifacts resulting from motion of subjects, facial expressions, talking, skin tone, and illumination variations. This paper proposes an efficient non-contact system based on a digital camera to track the cardiorespiratory signal from a number of subjects (up to six persons) at the same time with a new method for noise artifact removal. The proposed system relied on the physiological and physical effects as a result of the activity of the cardiovascular and respiratory systems, such as skin color changes and head motion. Since these effects are imperceptible to the human eye and highly affected by the noise variations, we used advanced signal and video processing techniques, including developing video magnification technique, complete ensemble empirical mode decomposition with adaptive noise, and canonical correlation analysis to extract the heart rate and respiratory rate from multiple subjects under the noise artifact assumptions. The experimental results of the proposed system had a significant correlation (Pearson's correlation coefficient = 0.9994, Spearman correlation coefficient = 0.9987, and root mean square error = 0.32) when compared with the conventional contact methods (pulse oximeter and piezorespiratory belt), which makes the proposed system a promising candidate for novel applications.

INDEX TERMS Cardiorespiratory signal, camera imaging-based methods, imaging photoplethysmography (iPPG), video magnification technique, complete ensemble EMD with adaptive noise, canonical correlation analysis, graphical user interface.

I. INTRODUCTION

Two critical physiological variables of heart rate and breathing rate are useful in the first instant of clinical interaction with patients and might be monitored continuously for hours or weeks if a patient is under intensive care. Long-term monitoring of individuals with chronic illnesses might occur in the home. In many situations, it would be desirable to measure cardiorespiratory data from multiple individuals and to not assume that each individual fills the frame of the camera. In some crisis situations, neonatal infants might be placed in pairs or even more inside incubators, without adequate instrumentation to monitor them all [1]. There are many potential applications outside clinical environments. Field triage with multiple wounded, security and quarantine check points and other crowded controlled areas are some

obvious examples. In these instances, people are standing or prone, with only modest movement. It would also be highly desirable for future robots to be able to read vital signs of any number of humans with whom they might interact.

Activity of both heart and lungs causes some physiological and physical effects on the human body, such as skin color change, heat patterns, arterial pulse motion, head oscillation and thorax motion. Although most of these effects are invisible to human operators due to limited spatiotemporal sensitivity of the human eye, they can be very useful in biomedical applications [2]–[5], when physiological signs, such as heart rate (HR), heart rate variability (HRV), respiration rate (RR), and blood oxygenation (SpO₂) must be remotely acquired.

Many technologies for remotely tracking the cardiorespiratory signal which contains important physiological signs

that have been proposed during the last decades, include technologies based on Doppler radar [6]–[11], thermal imaging [12]–[17], and capacitive coupled electrocardiography (ECG) measurement [18]–[21]. However, these technologies have been reported to be able to only extract the cardiorespiratory signal from a single subject at a time, and they are highly affected by noise artifacts particularly with a moving subject. In addition, these technologies need specialized hardware, which are somewhat expensive [22], [23].

Many researchers have shown that the cardiorespiratory signal can be remotely acquired from different types of camera sensors (e.g. video camera, Webcam, time of flight camera, Kinect etc.) by analyzing image sequences for single/multiple channels to reveal the cardiorespiratory signal either with a dedicated light source or using ambient illumination. Camera imaging-based technologies can be divided into two categories: imaging Photoplethysmography (iPPG) methods, which rely on optical properties of skin color changes; and motion-based methods, which rely on the mechanical activity of the heart and lungs. A comprehensive review of the remote monitoring technologies can be found in [22], [23]. As reported in a comprehensive review by Kranjec *et al.* [23], the cardiorespiratory signal for multiple subjects at a time could be acquired by using camera imaging. However, there was only one study by Poh *et al.* [24] that successfully extracted cardiorespiratory signal from three subjects simultaneously under a single scenario (stationary subjects). Furthermore, the cardiorespiratory signal is highly affected by noise artifacts (e.g. subject's motions, facial expressions, talking, skin tone and illumination variations); therefore, several studies proposed different algorithms to remove or reduce the noise artifacts. The major researches that used camera imaging-based technologies are reviewed and summarized in Table 1.

Most of the studies listed in Table 1 were limited to detecting physiological signs from a single subject with varying degrees of the noise artifacts immunity. Focusing on the lack of algorithms for tracking physiological signs from a number of subjects at a time and the noise artifact challenges, the current study has two contributions. The first contribution is to reveal the cardiorespiratory signal (HR and RR) from multiple subjects (up to 6 persons) based on both iPPG and head motion-based methods. The second contribution is to propose a new method for noise artifact reduction based on complete ensemble EMD with adaptive noise (CEEMDAN) and canonical correlation analysis (CCA) under different assumptions. Therefore, the proposed system may be of value for upcoming remote monitoring systems in biomedical, clinical and security applications.

II. METHODS AND PROCEDURES

A. ETHICAL CONSIDERATIONS

The research procedure described in this paper adhered to the ethical tenets of the Declaration of Helsinki (Finland 1964). It is part of a research protocol approved by the University

of South Australia Human Research Ethics Committee (Adelaide, South Australia, Protocol No. 0000034901), in which all of the participants who were recruited gave written informed consent after a full explanation of the research procedure before commencing the experiment.

B. SUBJECTS, VIDEO ACQUISITION AND VALIDATION

A group of eighteen healthy subjects (12 males and 6 females) between the ages of 6 and 50 years, with different skin tones were recruited to the experiment. The input videos were acquired by a digital camera (Nikon D5300) located at a distance of 3 meters from the subjects in outdoor and indoor environments. The input videos were captured for 20 sec at 60Hz and 30Hz frame rates with a resolution of 1920×1080. The subjects were instructed to breathe normally and to partake in two scenarios during videoing (stationary scenario and non-stationary scenario). All subjects in the stationary scenario were instructed to stay as still as possible in front of the camera, not talk and not make any facial expressions with normal breathing, whereas they were instructed to naturally move and rotate their faces, talking, blinking and making some facial expressions in the non-stationary scenario. The reference methods for monitoring of physiological signs (HR and RR) were measured using a finger pulse oximeter (Rossmax SA210) [33] and Piezo respiratory belt transducer (MLT1132) [34] and compared with the 20 sec signal recording obtained from the proposed system for validation purposes.

C. DATA ANALYSIS AND PROCESSING

The overall proposed system is composed of several main processing methods, including video magnification methods, face detection, CEEMDAN, CCA, component selection, frequency analysis and peak detection as shown in Fig. 1.

1) VIDEO MAGNIFICATION METHODS

- **Color Magnification Based-Method:** Skin color variations in the face caused by the cardiac pulse were magnified using Eulerian video magnification (EVM) [36]. To reduce the processing time, we applied the Lanczos resampling method [38] to reduce the size of the image sequences and magnified only the green (G) channel since this channel has been found to contain the strongest cardiac information signal [40]. The temporal band-pass filter processing is set to between 0.15 Hz- 3 Hz, corresponding to the anticipated range of the cardiorespiratory frequency band and then this band was magnified by 15x. The cardiorespiratory signal derived from the optical properties of skin color changes can be described as the iPPG signal.
- **Head Motion Magnification Based-Method:** Based on an efficient motion magnification method [43], the image sequences of the input video are converted from red green blue (RGB) colour space to $YCbCr$ colour space to separate the color data from the intensity

TABLE 1. A research review of the camera imaging- based technologies.

	Activity	Sensor type	Principle	The used technique	ROIs	Noise artifact	No. of subjects
Nakajima et al. [25]	Cardiac and respiratory	CCD	Motion- based method	OF	Entire body	*	1
Nakajima et al. [26]	Respiratory activity	CCD	Motion- based method	OF	Chest	*	1
Parra & Da Costa [27]	Cardiac activity	TV camera	Motion- based method	OF	Arm, wrist & neck	*	1
Poh et al. [24]	Cardiac and respiratory	Webcam	iPPG	ICA	Face	**	1, 3
Wiesner and Yaniv [28]	Respiratory	Webcam	Motion- based method	PCA	thoracic & abdominal	**	1
Lewandowska et al. [29]	Cardiac activity	Webcam	iPPG	PCA	face & forehead	*	1
Pursche et al. [30]	Cardiac activity	Webcam	iPPG	ICA	Forehead, nose & mouth	**	1
Scalise et al. [31]	Cardiac activity	Webcam	iPPG	ICA	forehead	**	1
Sun et al. [32]	Cardiac and respiratory	CMOS+ Webcam	iPPG	ICA	Face, forehead & hand	**	1
Penne et al. [35]	Respiratory activity	ToF camera	Motion- based method	Depth image sequence analysis	Thoracic & abdominal area	***	1
Falie et al [37]	Cardiac activity	Cell phone	iPPG	ICA	Face	**	1
Yu et al [39]	Cardiac activity	Webcam	iPPG	Single channel analysis + skin detections	face	***	1
Kwon et al. [41]	Cardiac activity	Cell phone	iPPG	Single channel analysis + skin detections	face	***	1
Bousefsaf et al. [42]	Cardiac activity	Webcam	iPPG	Single channel analysis + skin detections	face	***	1
Yu et al [44]	Respiratory activity	Kinect	Motion- based method analysis	Depth image sequence	Thoracic & abdominal	***	1
Xia, & Siochi [46]	Respiratory activity	Kinect	Motion- based method analysis	Depth image sequence	Thoracic & abdominal	***	1
Bernacchia et al. [47]	Cardiac and respiratory	Kinect	Motion- based method analysis	Depth info + ICA	Neck, chest and abdomen	***	1
De Haan & Jeanne [48]	Cardiac activity	CCD	iPPG	CHRO	Face	***	1
De Haan & Van Leest [50]	Cardiac activity	CCD	iPPG	PBV	Face	***	1
Li et al. [52]	Cardiac activity	iSight camera	iPPG	Single channel analysis	face	***	1
McDuff et al. [54]	Cardiac and respiratory	Digital camera	iPPG	Single/Multiple channel analysis	Face, forehead	**	1
Balakrishnan et al. [56]	Cardiac activity	Digital camera	Motion- based method analysis	Feature extraction + PCA	head	*	1
Shan & Yu [58]	Cardiac activity	Cell phone	Motion- based method analysis	Feature extraction + ICA	head	*	1
Irani et al. [59]	Cardiac activity	Webcam	Motion- based method analysis	Feature extraction + PCA	head	**	1
Feng et al. [61]	Cardiac activity	Webcam	iPPG	ICA	forehead	**	1
Tarassenko et al. [62]	Cardiac and respiratory	CCD	iPPG	RGB channel analysis + AR model	Forehead or check	**	1
Alnaji & Chahl [63]	Respiratory activity	CMOS	Motion- based method	Video magnification+ Frame subtraction	Chest	**	1
Hsu et al. [64]	Cardiac activity	CMOS	iPPG	SVR	face	***	1
Feng et al. [65]	Cardiac activity	Webcam	iPPG	ICA/ CHRO	face	***	1
Chen et al. [66]	Cardiac activity	Digital camera	iPPG	Multiple channel analysis + GRD	Face, forehead & check	***	1
Lin et al. [73]	Cardiac activity	Digital camera	iPPG	Single channel analysis +EEMD	forehead	***	1
Wiede et al. [75]	Cardiac activity	CCD	iPPG	ICA/PCA	Face & forehead	**	1
Cheng et al. [76]	Cardiac activity	Webcam	iPPG	JBSS + EEMD	Face	***	1
He et al. [77]	Cardiac activity	Digital camera	Motion- based method	Video magnification	Wrist	*	1
Alnaji & Chahl [78]	Cardiac activity	CMOS	Motion- based method	Video magnification+ Frame subtraction	Wrist, arm, neck and leg	*	1
Wang et al. [79]	Cardiac activity	CCD	iPPG	2SR	Face & forehead	***	1
Wang et al. [80]	Cardiac activity	CCD	iPPG	POS	Face	***	1
Alnaji & Chahl [81]	Cardiac activity	CMOS	Motion- based method	Video magnification + Frame subtraction	Head	**	1

Note: AR= auto-regressive; CCD= charge-coupled device; CHRO= chrominance; CMOS= complementary metal-oxide-semiconductor; EEMD= ensemble empirical mode decomposition; GRD= green/red difference; ICA= independent component analysis; JBSS= joint blind source separation; OF= optical flow; PBV= blood volume pulse vector; PCA= principle component analysis; POS= plane orthogonal to skin; SVR= support vector regression; 2SR= spatial subspace rotation; ToF= time of flight.

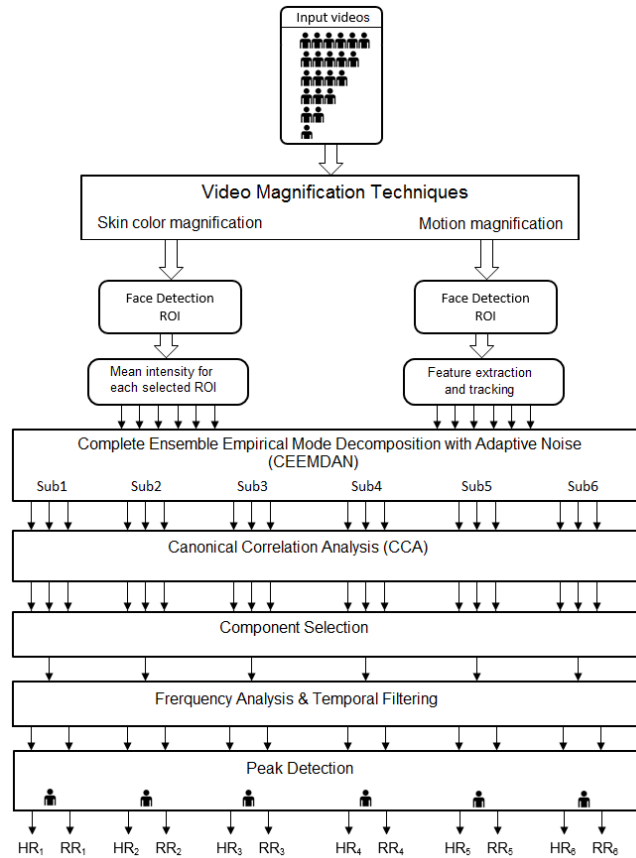


FIGURE 1. Processing stages overview of the proposed system.

data. Only the Y channel was used and downsized to reduce the processing time. The Y channel was then decomposed into different spatial frequency bands using wavelet pyramids followed by a temporal band-pass filter of 0.15 Hz- 3 Hz to extract frequency bands of interest. The filtered signal was then magnified by 15x.

2) FACE DETECTION AND FEATURE EXTRACTION

Based on the video obtained from the color magnification-based method, we applied an effective face detection method proposed by Liao *et al.* [45], which can deal with challenges associated with unconstrained faces (e.g. faces in a crowd, face rotation, inclined or angled faces) to obtain a number of regions of interest (ROI) according to the number of subjects in the input video. We also eliminated the eyes and mouth regions from each ROI to reduce the noise artifacts resulting from blinking and talking during the measurements. For each ROI, the time-series iPPG signal, $i_c(t)$, was obtained by averaging all the image pixel values within the facial ROI as follows:

$$i_c(t) = \frac{\sum_{x,y \in ROI} I(x, y, t)}{|ROI_1|} \quad (1)$$

where $I(x, y)$ is the intensity pixel value at image location (x, y) , at time (t) and $|ROI_1|$ is the size of the facial ROI

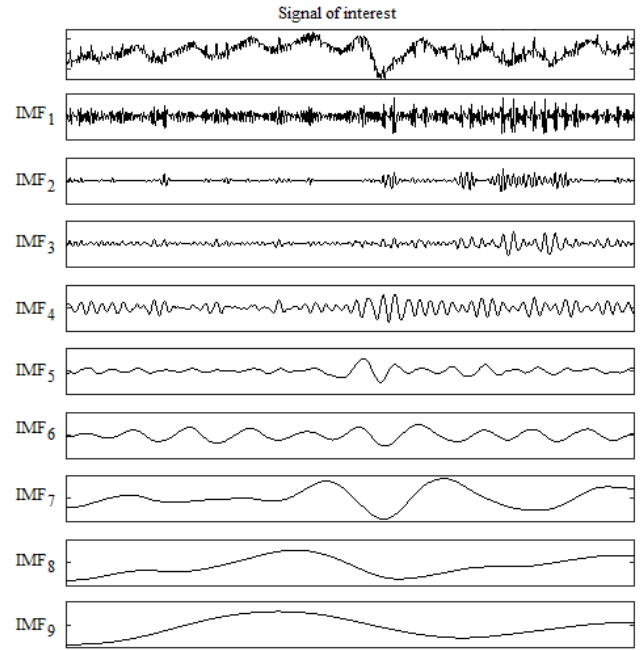


FIGURE 2. IMFs of the CEEMDAN for the signal of interest.

for the subject 1. The observed signals from six subjects are denoted by $i_{c1}(t), i_{c2}(t), \dots, i_{c6}(t)$ respectively.

Based on the video obtained from the motion magnification method, we also applied Liao's method for detecting faces and selected only small region on the forehead (rectangle region). Then, we selected a single feature point in the centre of the rectangle for extracting head motion. The selected feature point has two components in both the vertical and horizontal axis. The vertical components for all image sequence were only chosen to obtain time-series signal $i_m(t)$ resulting from head motion. The observed signals from six subject are denoted by $i_{m1}(t), i_{m2}(t), \dots, i_{m6}(t)$ respectively.

3) COMPLETE ENSEMBLE EMD WITH ADAPTIVE NOISE

The empirical mode decomposition (EMD) [49] is one of the most effective signal processing methods for removal of noise artifacts from biomedical signals (e.g. removal of noise artifacts from the ECG data [51], removal the noise artifacts from the EMG data [53] and removal of the muscle artifacts from the EEG data [55]). The EMD is a time-frequency analysis method for adaptively decomposing a given non-linear and/or non-stationary signal into a set of amplitude and frequency components (multichannel signals), called intrinsic mode functions (IMFs). Later, a noise-assisted version, called ensemble EMD, was proposed by Wu and Huang [57] to reduce the mode mixing problem associated with the EMD. However, ensemble EMD still has some limitations, including residual noise, reconstruction error and modes for different realizations of signal plus noise [60]. A recent improved version of the ensemble EMD, namely the CEEMDAN method, has been proposed by Colominas *et al.* [60] to

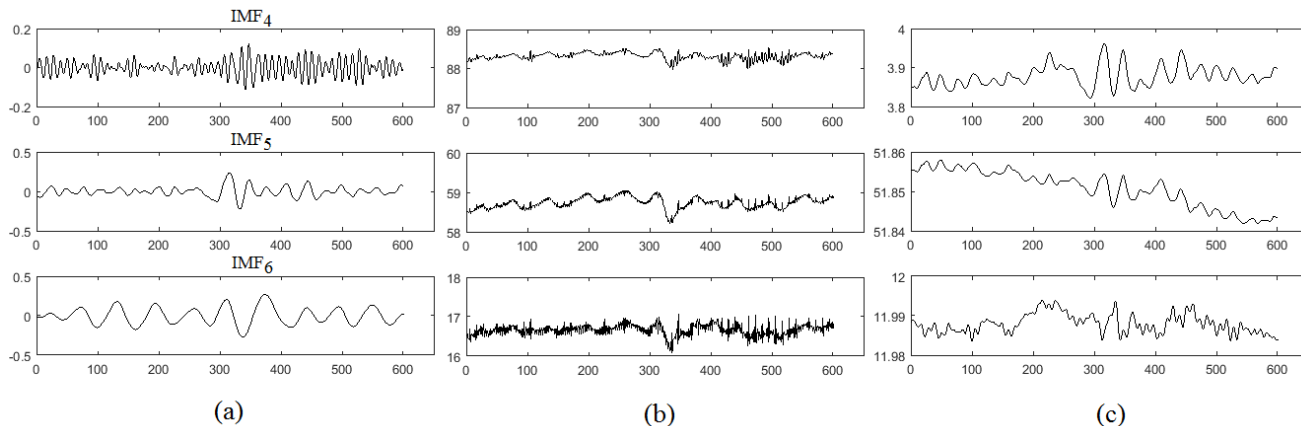


FIGURE 3. The CCA method (a) The selected IMFs components (S) (b) Transformation $[x = W \cdot S]$, where W is an un-mixing matrix and (c) CCA outputs $[y = CCA(x)]$.

solve the problems associated with the ensemble EMD. The CEEMDAN method can efficiently decompose the signal of interest into a set of IMFs with less noise and more physical meaning.

The signal of interests, $i_c(t)$ generated from the first kind of magnification, and $i_m(t)$ generated from the second kind of magnification for each subject, can be converted into multichannel signals based on CEEMDAN decomposition as follows: [60]

$$i_c(t), i_m(t) = \sum_{m=1}^M \tilde{d}_m + r_M \quad (2)$$

where \tilde{d}_m is the m^{th} mode of the signal of interest obtained by averaging the corresponding CEEMDAN modes, r_M is m^{th} residue obtained from $(r_{(m-1)} - \tilde{d}_m)$ and M is the total number of modes.

An example of nine multichannel signal IMFs of the signal of interest, based on CEEMDAN decomposition with 100 realizations and iterations, is given in Fig. 2.

4) CANONICAL CORRELATION ANALYSIS

The CCA [67] is also an effective signal processing method that can be used as a blind source separation (BSS), to separate a number of mixed signals [68], [69] and remove the noise artifact from the biomedical signals [70]–[72].

To understand how CCA operates as a BSS, let j and k be two multi-dimensional random signals. Consider the linear combinations of these signals, known as the canonical variates as follows [74]:

$$j = W_j^T [j - \bar{j}], \quad k = W_k^T [k - \bar{k}] \quad (3)$$

where W_j and W_k are weighting matrices of j and k . The correlation, ρ , between these linear combinations is given by:

$$\rho = \frac{W_j^T C_{jk} W_k}{\sqrt{W_j^T C_{jj} W_j W_k^T C_{kk} W_k}} \quad (4)$$

where C_{jj} and C_{kk} are the nonsingular within-set covariance matrices and C_{jk} is the between-sets covariance matrix.

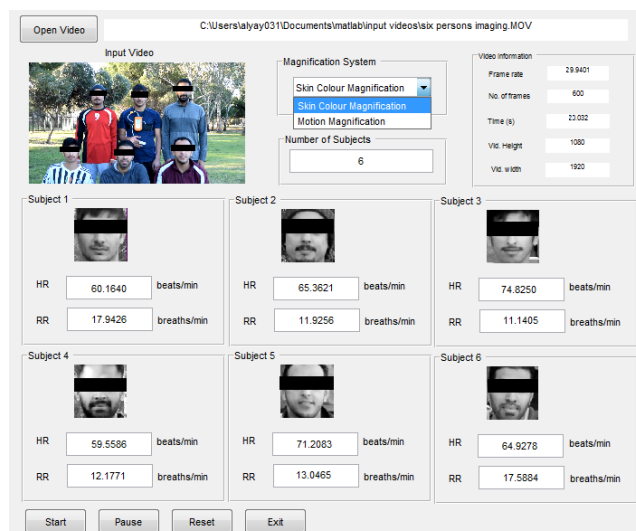


FIGURE 4. The GUI main panel of the proposed system.

The largest canonical variates can be found with the maximum value of ρ with respect to W_j and W_k .

We applied the CCA method on three IMFs components which have the best frequency bands of interest (IMF4, IMF5 and IMF6 since the frequency band fall within 0.15- 3 Hz in these components) as shown in Fig. 3.

Each signal of interest, $i_c(t)$, $i_m(t)$, is converted into a multichannel signal (S), using the CEEMDAN method. The IMFs determined to be outside frequency bands of interest are removed and then, the remaining IMFs determined to be within frequency bands of interest are used as inputs with the un-mixing matrix W of the CCA method. The original multichannel signal \tilde{S} , is then reconstructed without unwanted IMFs, using the inverse of the un-mixing matrix W^{-1} . Now, the target signal of interest, $\tilde{i}_c(t)$, $\tilde{i}_m(t)$, without the noise artifacts, can be reconstructed by adding the new IMF components in the \tilde{S} matrix. We selected the most periodic components with the highest power spectra as the signal of interest.

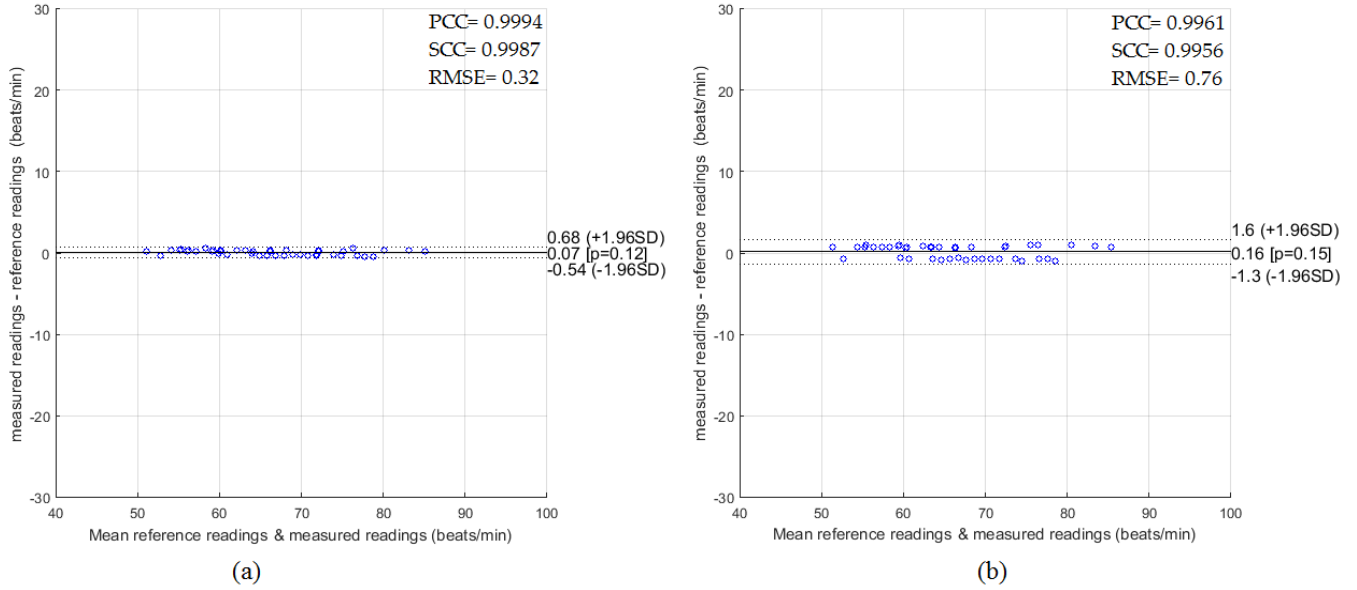


FIGURE 5. The Bland-Altman plots and the statistics for HR measurements under the stationary scenario using (a) iPPG-based method, (b) motion-based method.

5) FREQUENCY ANALYSIS AND TEMPORAL FILTERING

Frequency analysis based on Fast Fourier Transformer (FFT) was applied to transform $\tilde{i}_c(t)$, $\tilde{i}_m(t)$, from the time domain to the frequency domain followed by two 5th order Butterworth band-pass filters with different frequency bands to separate the cardiac signal from the respiratory signal. The selected band-pass frequencies were of 0.5-3Hz that correspond to HR range between 30-180 beats/min, and 0.15-0.5Hz that correspond to RR range between 9-30 breaths/min. The inverse FFT was severally applied to the filtered signals to obtain the time-series cardiac and respiratory signals respectively.

6) PEAK DETECTION

The peak detection method was used to only pick the positive peaks of the acquired signals and determine the number of peaks and their locations. The peak detection was accomplished using “*findpeaks*” function in the Matlab software. Since both peaks and their locations were detected, we could measure HR and RR per minute using the following equation:

$$HR, RR = \frac{60k}{L} \quad (5)$$

where k is the number of peaks in the acquired signal and L is the time of the video in seconds. In addition, our proposed system can estimate other physiological signs by measuring the period between two consecutive peaks, which are called heart rate variability (HVR) (cycle length between two consecutive cardiac beats) and the respiratory cycle (a single cycle of inhalation and exhalation).

III. GRAPHICAL USER INTERFACE (GUI)

A GUI model was implemented in the Matlab software to allow the user to load video data, select the magnification type and execute the algorithm. The proposed GUI provides an

easy tool to see video information, number of subjects in each input video and subject’s faces to enable the user to recognize the HR and RR readings for each subject. Fig. 4 shows the GUI main panel of the proposed system.

IV. EXPERIMENTAL RESULTS AND DISCUSSION

A. STATIONARY SCENARIO

In this scenario, all subjects were instructed to stay as still as possible in front of the camera and not talk or make any facial expressions with normal breathing. The results were obtained for a subject from a group of persons when different assumptions were considered (e.g. persons with different ages, skin tone, and videoing with different lighting conditions). The Bland-Altman method [82] was used to assess the level of agreement between the experimental results obtained from the proposed system and those obtained from the reference methods. Furthermore, the relationship between the results was evaluated using Pearson’s correlation coefficient (PCC), Spearman correlation coefficient (SCC) and root mean square error (RMSE). The Bland-Altman plots and the statistics for HR measurements based on the magnification type is shown in Fig. 5.

It is apparent from Fig. 5 (a) that the iPPG-based method under the stationary scenario has a strong correlation and statistics (PCC=0.9994, SCC=0.9987 and REME=0.32 beats/min) between the HR estimates and the HR reference values, while the statistics slightly changed to 0.9961, 0.9956 and 0.76 beats/min respectively when the motion-based method was used instead as shown in Fig. 5 (b).

The statistics of the RR measurements based on iPPG-based method shown in Fig. 6 (a) also presented a higher correlation with the statistics (PCC=0.9893, SCC=0.9874 and RMSE=0.32 breaths/min) than those

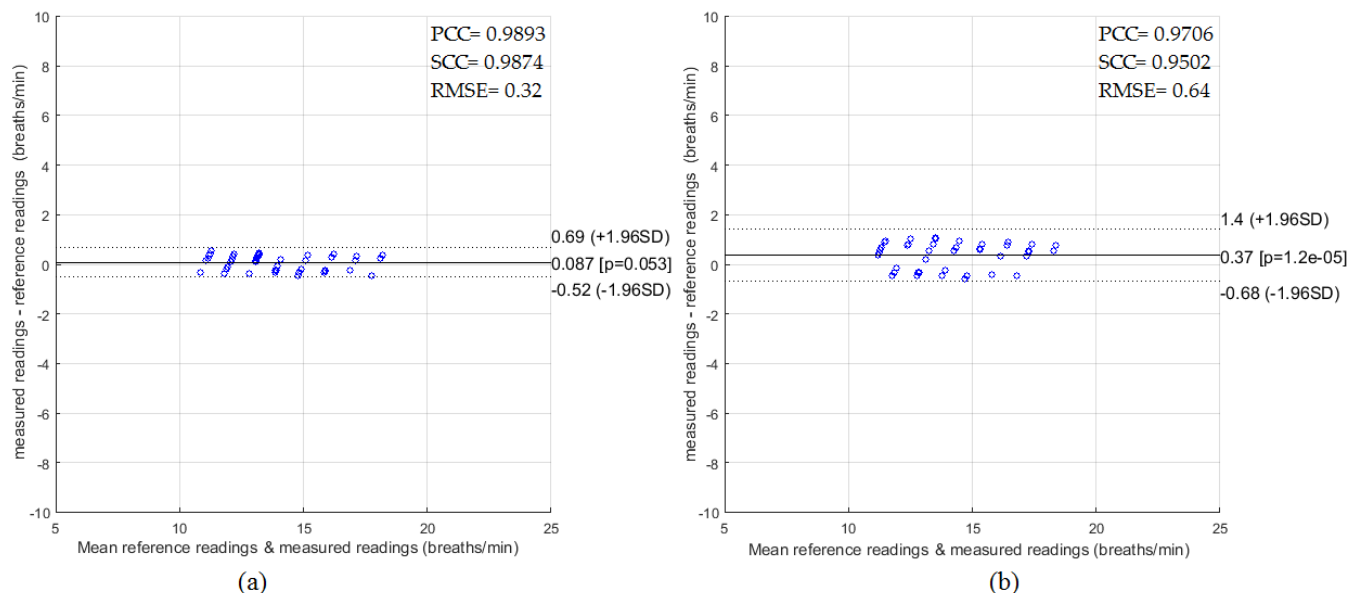


FIGURE 6. The Bland-Altman plots and the statistics for RR measurements under the stationary scenario using (a) iPPG-based method, (b) motion-based method.

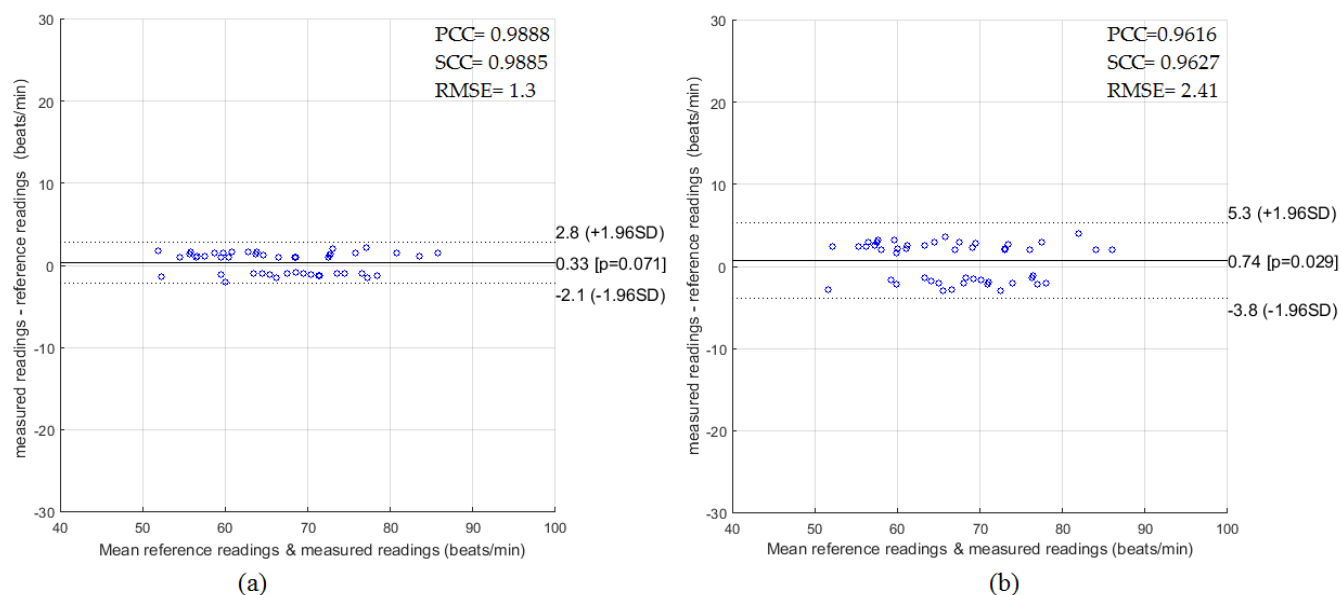


FIGURE 7. The Bland-Altman plots and the statistics for HR measurements under the non-stationary scenario using (a) iPPG-based method, (b) motion-based method.

obtained from the motion-based method (PCC=0.9706, SCC=0.9502 and RMSE=0.64 breaths/min) shown in Fig. 6 (b). Therefore, our system presented a high feasibility and tolerance of noise artifacts for both methods (iPPG and motion) when the subjects were stationary.

B. NON-STATIONARY SCENARIO

In this scenario, all subjects were instructed to move and rotate their faces by talking and making some facial expressions. The statistical agreement of the HR measurements using Bland-Altman plots for both methods against the reference method is shown in Fig. 7 (a) and (b).

The results from Fig. 7 (a) shows a high degree of correlation between physiological measurements based on iPPG for moving subjects with statistics of 0.9888, 0.9885 and 1.3 beats/min for PCC, SCC and RMSE respectively, while the results obtained from the motion-based method show less correlation with statistics of 0.9616, 0.9627 and 2.41 beats/min respectively as shown in Fig. 7 (b).

The RR measurements for moving subjects based on the iPPG-based method shown in Fig. 8 (a), has correlations (PCC=0.8455, SCC=0.8367 and RMSE=1.25 breaths/min) which are substantially better than those obtained from the motion-based method (PCC=0.6209, SCC=0.5963 and

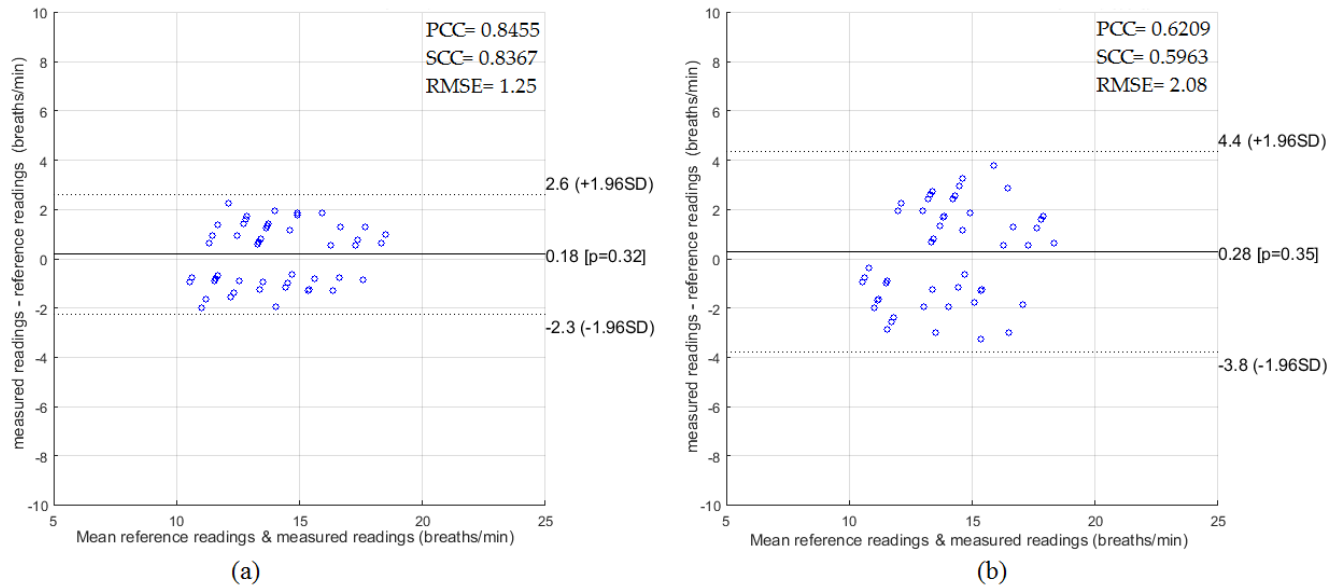


FIGURE 8. The Bland-Altman plots and the statistics for RR measurements under the non-stationary scenario using (a) iPPG-based method, (b) motion-based method.

RMSE=2.08 breaths/min) as shown in Fig. 8 (b). The motion-based method seems to be affected by noise variations with non-stationary subjects, when compared to the iPPG-based method. Although some studies [56], [58], [59], [81] have reported that the head motion-based method is more efficient than iPPG-based method for subjects with different skin tone, illumination conditions and unclear ROI (e.g. videos captured from the back of the head or covered with a mask). Since it depends on motion analysis more than skin color analysis, the head motion-based method is still affected by noise variations with moving subjects, when compared to the iPPG-based method.

The imaging-based methods based on both color and motion analysis, seem to be an attractive candidate for future applications when noise and motion artifact sensitivity cannot be solved by a single method.

V. CONCLUSION

In this paper, we propose a new non-contact monitoring system to extract HR and RR from multiple subjects with noise artifact removal. The proposed system used the developing video magnification method to amplify the imperceptible effects caused by cardiorespiratory activity, such as skin color and head motion to extract the cardiorespiratory signal followed by a new noise removal method based on a combination of CEEMDAN and CCA to remove the noise artifacts resulting from the subject's motions, facial expressions, talking, skin tone and illumination variations. The experimental results showed that the proposed system has strong correlation in agreement with the reference measurements in both the stationary and non-stationary scenarios. Further studies with larger numbers of subjects with different scenarios are clearly needed to confirm these outcomes. Real-time and long-term monitoring with different

assumptions using different types of cameras are the main considerations in future work, in order to increase system's reliability.

ACKNOWLEDGEMENTS

The authors thank Titilayo Ogunwa for assistance in preparing the manuscript.

REFERENCES

- [1] H. O. Amadi, "Neonatal thermoneutrality in a tropical climate," in *Current Topics in Tropical Medicine*. Rijeka, Croatia: InTech, 2012, p. 535.
- [2] C. Brüser, C. H. Antink, T. Wartzek, M. Walter, and S. Leonhardt, "Ambient and unobtrusive cardiorespiratory monitoring techniques," *IEEE Rev. Biomed. Eng.*, vol. 8, pp. 30–43, 2015.
- [3] A. A. Alnaji, K. Gibson, S.-H. Lee, and J. Chahl, "Real time apnoea monitoring of children using the microsoft Kinect sensor: A pilot study," *Sensors*, vol. 17, no. 2, p. 286, 2017.
- [4] A. Alnaji, K. Gibson, and J. Chahl, "Remote sensing of physiological signs using a machine vision system," *J. Med. Eng. Technol.*, vol. 41, no. 5, pp. 396–405, 2017.
- [5] J. Allen, "Photoplethysmography and its application in clinical physiological measurement," *Physiol. Meas.*, vol. 28, no. 3, p. R1-39, 2007.
- [6] V. Vasu, C. Heneghan, T. Arumugam, and S. Sezer, "Signal processing methods for non-contact cardiac detection using Doppler radar," in *Proc. IEEE Workshop Signal Process. Syst. (SIPS)*, Oct. 2010, pp. 368–373.
- [7] H. Tan, D. Qiao, and Y. Li, "Non-contact heart rate tracking using Doppler radar," in *Proc. Int. Conf. Syst. Informat. (ICSAI)*, 2012, pp. 1711–1714.
- [8] L. Scalise, I. Ercoli, P. Marchionni, and E. P. Tomasini, "Measurement of respiration rate in preterm infants by laser Doppler vibrometry," in *Proc. IEEE Int. Workshop Med. Meas. Appl. (MeMeA)*, Oct. 2011, pp. 657–661.
- [9] L. Scalise, A. De Leo, V. M. Primiani, P. Russo, D. Shahu, and G. Cerri, "Non contact monitoring of the respiration activity by electromagnetic sensing," in *Proc. IEEE Int. Workshop Med. Meas. Appl. (MeMeA)*, Oct. 2011, pp. 418–422.
- [10] O. B. Lubecke, P.-W. Ong, and V. Lubecke, "10 GHz Doppler radar sensing of respiration and heart movement," in *Proc. IEEE 28th Annu. Northeast Bioeng. Conf.*, Sep. 2002, pp. 55–56.
- [11] W. Hu, Z. Zhao, Y. Wang, H. Zhang, and F. Lin, "Noncontact accurate measurement of cardiopulmonary activity using a compact quadrature Doppler radar sensor," *IEEE Trans. Biomed. Eng.*, vol. 61, no. 3, pp. 725–735, Mar. 2014.

- [12] M. Yang, Q. Liu, T. Turner, and Y. Wu, "Vital sign estimation from passive thermal video," in *Proc. IEEE Conf. Comput. Vis. Pattern Recognit. (CVPR)*, Jun. 2008, pp. 1–8.
- [13] G. F. Lewis, R. G. Gatto, and S. W. Porges, "A novel method for extracting respiration rate and relative tidal volume from infrared thermography," *Psychophysiology*, vol. 48, no. 7, pp. 877–887, 2011.
- [14] M. Garbey, N. Sun, A. Merla, and I. Pavlidis, "Contact-free measurement of cardiac pulse based on the analysis of thermal imagery," *IEEE Trans. Biomed. Eng.*, vol. 54, no. 8, pp. 1418–1426, Aug. 2007.
- [15] J. Fei and I. Pavlidis, "Thermistor at a distance: Unobtrusive measurement of breathing," *IEEE Trans. Biomed. Eng.*, vol. 57, no. 4, pp. 988–998, Apr. 2010.
- [16] S. Y. Chekmenev, H. Rara, and A. A. Farag, "Non-contact, wavelet-based measurement of vital signs using thermal imaging," in *Proc. 1st Int. Conf. Graph., Vis., Image Process. (GVIP)*, Cairo, Egypt, 2005, pp. 107–112.
- [17] S. Y. Chekmenev, A. A. Farag, W. M. Miller, E. A. Essock, and A. Bhatnagar, "Multiresolution approach for noncontact measurements of arterial pulse using thermal imaging," in *Augmented Vision Perception in Infrared*. Berlin, Germany: Springer, 2009, pp. 87–112.
- [18] R. Prance *et al.*, "An ultra-low-noise electrical-potential probe for human-body scanning," *Meas. Sci. Technol.*, vol. 11, no. 3, p. 291, 2000.
- [19] R. J. Prance, S. T. Beardsmore-Rust, P. Watson, C. J. Harland, and H. Prance, "Remote detection of human electrophysiological signals using electric potential sensors," *Appl. Phys. Lett.*, vol. 93, no. 3, p. 033906, 2008.
- [20] A. E. Mahdi and L. Faggion, "Non-contact biopotential sensor for remote human detection," *J. Phys. Conf. Ser.*, vol. 307, no. 1, p. 012056, 2011.
- [21] C. Harland, T. Clark, and R. Prance, "Electric potential probes-new directions in the remote sensing of the human body," *Meas. Sci. Technol.*, vol. 13, no. 2, p. 163, 2001.
- [22] A. Alnaji, K. Gibson, S.-H. Lee, and J. Chahl, "Monitoring of cardiorespiratory signal: Principles of remote measurements and review of methods," *IEEE Access*, vol. 5, pp. 15776–15790, 2017.
- [23] J. Kranjec, S. Beguš, G. Geršak, and J. Drnovšek, "Non-contact heart rate and heart rate variability measurements: A review," *Biomed. Signal Process. Control*, vol. 13, pp. 102–112, Sep. 2014.
- [24] M.-Z. Poh, D. J. McDuff, and R. W. Picard, "Non-contact, automated cardiac pulse measurements using video imaging and blind source separation," *Opt. Exp.*, vol. 18, no. 10, pp. 10762–10774, 2010.
- [25] K. Nakajima, A. Osa, and H. Miike, "A method for measuring respiration and physical activity in bed by optical flow analysis," in *Proc. IEEE 19th Annu. Int. Conf. Eng. Med. Biol. Soc.*, Oct./Nov. 1997, pp. 2054–2057.
- [26] K. Nakajima, Y. Matsumoto, and T. Tamura, "Development of real-time image sequence analysis for evaluating posture change and respiratory rate of a subject in bed," *Physiol. Meas.*, vol. 22, no. 3, pp. 21–28, 2001.
- [27] J. E. Parra and G. Da Costa, "Optical remote sensing of heartbeats," *Proc. SPIE*, vol. 4368, pp. 113–121, Aug. 2001.
- [28] S. Wiesner and Z. Yaniv, "Monitoring patient respiration using a single optical camera," in *Proc. 29th Annu. Int. Conf. IEEE Eng. Med. Biol. Soc. (EMBS)*, Aug. 2007, pp. 2740–2743.
- [29] M. Lewandowska, J. Rumiński, T. Kocejko, and J. Nowak, "Measuring pulse rate with a webcam—A non-contact method for evaluating cardiac activity," in *Proc. Federated Conf. Comput. Sci. Inf. Syst. (FedCSIS)*, 2011, pp. 405–410.
- [30] T. Pursche, J. Krajewski, and R. Moeller, "Video-based heart rate measurement from human faces," in *Proc. IEEE Int. Conf. Consum. Electron. (ICCE)*, Jan. 2012, pp. 544–545.
- [31] L. Scalise, N. Bernacchia, I. Ercoli, and P. Marchionni, "Heart rate measurement in neonatal patients using a webcam," in *Proc. IEEE Int. Symp. Med. Meas. Appl. Proc. (MeMeA)*, May 2012, pp. 1–4.
- [32] Y. Sun, S. Hu, V. Azorin-Peris, S. Greenwald, J. Chambers, and Y. Zhu, "Motion-compensated noncontact imaging photoplethysmography to monitor cardiorespiratory status during exercise," *J. Biomed. Opt.*, vol. 16, no. 7, p. 077010-9, 2011.
- [33] *Rossmax Pulse Oximeter*. Accessed: Jul. 1, 2017. [Online]. Available: <https://www.medshop.com.au/products/rossmax-hand-held-pulse-oximeter-sa210>
- [34] *ADInstruments. MLT1132 Piezo Respiratory Belt Transducer*. Accessed: Jul. 1, 2017. [Online]. Available: <http://m-cdn.adinstruments.com/product-data-cards/MLT1132-DCW-15A.pdf>
- [35] J. Penne, C. Schaller, J. Hornegger, and T. Kuwert, "Robust real-time 3D respiratory motion detection using time-of-flight cameras," *Int. J. Comput. Assist. Radiol. Surg.*, vol. 3, no. 5, pp. 427–431, 2008.
- [36] H.-Y. Wu, M. Rubinstein, E. Shih, J. V. Guttag, F. Durand, and W. T. Freeman, "Eulerian video magnification for revealing subtle changes in the world," *ACM Trans. Graph.*, vol. 31, no. 4, p. 65, 2012.
- [37] D. Falie, L. David, and M. Ichim, "Statistical algorithm for detection and screening sleep apnea," in *Proc. Int. Symp. Signals, Circuits Syst. (ISSCS)*, 2009, pp. 1–4.
- [38] B. Madhukar and R. Narendra, "Lanczos resampling for the digital processing of remotely sensed images," in *Proc. Int. Conf. VLSI, Commun. Adv. Devices, Signals Syst. Netw. (VCASAN)*, 2013, pp. 403–411.
- [39] M.-C. Yu, H. Wu, J.-L. Liou, M.-S. Lee, and Y.-P. Hung, "Breath and position monitoring during sleeping with a depth camera," in *Proc. Int. Conf. Health Informat.*, 2012, pp. 12–22.
- [40] W. Verkruysse, L. O. Svaasand, and J. S. Nelson, "Remote plethysmographic imaging using ambient light," *Opt. Exp.*, vol. 16, no. 26, pp. 21434–21445, 2008.
- [41] S. Kwon, H. Kim, and K. S. Park, "Validation of heart rate extraction using video imaging on a built-in camera system of a smartphone," in *Proc. Annu. Int. Conf. IEEE Eng. Med. Biol. Soc. (EMBC)*, San Diego, CA, USA, May 2012, pp. 2174–2177.
- [42] F. Bousefsaf, C. Maoui, and A. Pruski, "Continuous wavelet filtering on webcam photoplethysmographic signals to remotely assess the instantaneous heart rate," *Biomed. Signal Process. Control*, vol. 8, no. 6, pp. 568–574, 2013.
- [43] A. Al-Naji, S.-H. Lee, and J. Chahl, "Quality index evaluation of videos based on fuzzy interface system," *IET Image Process.*, vol. 11, no. 5, pp. 292–300, 2017.
- [44] M.-C. Yu, J.-L. Liou, S.-W. Kuo, M.-S. Lee, and Y.-P. Hung, "Non-contact respiratory measurement of volume change using depth camera," in *Proc. Annu. Int. Conf. IEEE Eng. Med. Biol. Soc. (EMBC)*, Nov. 2012, pp. 2371–2374.
- [45] S. Liao, A. K. Jain, and S. Z. Li, "A fast and accurate unconstrained face detector," *IEEE Trans. Pattern Anal. Mach. Intell.*, vol. 38, no. 2, pp. 211–223, Feb. 2016.
- [46] J. Xia and R. A. Siochi, "A real-time respiratory motion monitoring system using KINECT: Proof of concept," *Med. Phys.*, vol. 39, no. 5, pp. 2682–2685, 2012.
- [47] N. Bernacchia, L. Scalise, L. Casacanditella, I. Ercoli, P. Marchionni, and E. P. Tomasini, "Non contact measurement of heart and respiration rates based on Kinect," in *Proc. IEEE Int. Symp. Med. Meas. Appl. (MeMeA)*, Jun. 2014, pp. 1–5.
- [48] G. de Haan and V. Jeanne, "Robust pulse rate from chrominance-based rPPG," *IEEE Trans. Biomed. Eng.*, vol. 60, no. 10, pp. 2878–2886, Oct. 2013.
- [49] N. E. Huang *et al.*, "The empirical mode decomposition and the Hilbert spectrum for nonlinear and non-stationary time series analysis," *Philos. Trans. Roy. Soc. London A, Math. Phys. Sci.*, vol. 454, no. 1971, pp. 903–995, 1998.
- [50] G. De Haan and A. Van Leest, "Improved motion robustness of remote-PPG by using the blood volume pulse signature," *Physiol. Meas.*, vol. 35, no. 9, p. 1913, 2014.
- [51] M. Blanco-Velasco, B. Weng, and K. E. Barner, "ECG signal denoising and baseline wander correction based on the empirical mode decomposition," *Comput. Biol. Med.*, vol. 38, no. 1, pp. 1–13, Jan. 2008.
- [52] X. Li, J. Chen, G. Zhao, and M. Pietikainen, "Remote heart rate measurement from face videos under realistic situations," in *Proc. IEEE Conf. Comput. Vis. Pattern Recognit.*, Jun. 2014, pp. 4264–4271.
- [53] X. Zhang and P. Zhou, "Filtering of surface EMG using ensemble empirical mode decomposition," *Med. Eng. Phys.*, vol. 35, no. 4, pp. 537–542, 2013.
- [54] D. McDuff, S. Gontarek, and R. W. Picard, "Improvements in remote cardiopulmonary measurement using a five band digital camera," *IEEE Trans. Biomed. Eng.*, vol. 61, no. 10, pp. 2593–2601, Oct. 2014.
- [55] X. Chen, A. Liu, J. Chiang, Z. J. Wang, M. J. McKeown, and R. K. Ward, "Removing muscle artifacts from EEG data: Multichannel or single-channel techniques?" *IEEE Sensors J.*, vol. 16, no. 7, pp. 1986–1997, Apr. 2016.
- [56] G. Balakrishnan, F. Durand, and J. Guttag, "Detecting pulse from head motions in video," in *Proc. IEEE Conf. Comput. Vis. Pattern Recognit. (CVPR)*, Jun. 2013, pp. 3430–3437.
- [57] Z. Wu and N. E. Huang, "Ensemble empirical mode decomposition: A noise-assisted data analysis method," *Adv. Adapt. Data Anal.*, vol. 1, no. 1, pp. 1–41, 2008.

- [58] L. Shan and M. Yu, "Video-based heart rate measurement using head motion tracking and ICA," in *Proc. 6th Int. Congr. Image Signal Process. (CISP)*, 2013, pp. 160–164.
- [59] R. Irani, K. Nasrollahi, and T. B. Moeslund, "Improved pulse detection from head motions using DCT," in *Proc. Int. Conf. Comput. Vis. Theory Appl. (VISAPP)*, 2014, pp. 118–124.
- [60] M. A. Colominas, G. Schlotthauer, and M. E. Torres, "Improved complete ensemble EMD: A suitable tool for biomedical signal processing," *Biomed. Signal Process. Control*, vol. 14, pp. 19–29, Nov. 2014.
- [61] L. Feng, L.-M. Po, X. Xu, and Y. Li, "Motion artifacts suppression for remote imaging photoplethysmography," in *Proc. 19th Int. Conf. Digit. Signal Process. (DSP)*, 2014, pp. 18–23.
- [62] L. Tarassenko, M. Villarroya, A. Guazzi, J. Jorge, D. Clifton, and C. Pugh, "Non-contact video-based vital sign monitoring using ambient light and auto-regressive models," *Physiol. Meas.*, vol. 35, no. 5, p. 807, 2014.
- [63] A. Alnaji and J. Chahl, "Remote respiratory monitoring system based on developing motion magnification technique," *Biomed. Signal Process. Control*, vol. 29, pp. 1–10, Aug. 2016.
- [64] Y. Hsu, Y.-L. Lin, and W. Hsu, "Learning-based heart rate detection from remote photoplethysmography features," in *Proc. IEEE Int. Conf. Acoust., Speech Signal Process. (ICASSP)*, May 2014, pp. 4433–4437.
- [65] L. Feng, L. M. Po, X. Xu, Y. Li, and R. Ma, "Motion-resistant remote imaging photoplethysmography based on the optical properties of skin," *IEEE Trans. Circuits Syst. Video Technol.*, vol. 25, no. 5, pp. 879–891, May 2015.
- [66] D.-Y. Chen *et al.*, "Image sensor-based heart rate evaluation from face reflectance using Hilbert–Huang transform," *IEEE Sensors J.*, vol. 15, no. 1, pp. 618–627, Jan. 2015.
- [67] D. R. Hardoon, S. Szedmak, and J. Shawe-Taylor, "Canonical correlation analysis: An overview with application to learning methods," *Neural Comput.*, vol. 16, no. 12, pp. 2639–2664, 2004.
- [68] W. Liu, D. P. Mandic, and A. Cichocki, "Analysis and online realization of the CCA approach for blind source separation," *IEEE Trans. Neural Netw.*, vol. 18, no. 5, pp. 1505–1510, Sep. 2007.
- [69] Y.-O. Li, T. Adali, W. Wang, and V. D. Calhoun, "Joint blind source separation by multiset canonical correlation analysis," *IEEE Trans. Signal Process.*, vol. 57, no. 10, pp. 3918–3929, Oct. 2009.
- [70] J. Gao, C. Zheng, and P. Wang, "Online removal of muscle artifact from electroencephalogram signals based on canonical correlation analysis," *Clin. EEG Neurosci.*, vol. 41, no. 1, pp. 53–59, 2010.
- [71] W. De Clercq, A. Vergult, B. Vanrumste, W. Van Paesschen, and S. Van Huffel, "Canonical correlation analysis applied to remove muscle artifacts from the electroencephalogram," *IEEE Trans. Biomed. Eng.*, vol. 53, no. 12, pp. 2583–2587, Nov. 2006.
- [72] A. Ali, P. G. Asanka, and C. Javaan, "Remote monitoring of cardiorespiratory signals from a hovering unmanned aerial vehicle," *Biomed. Eng. Online*, vol. 16, no. 1, p. 101, 2017.
- [73] K.-Y. Lin, D.-Y. Chen, and W.-J. Tsai, "Face-based heart rate signal decomposition and evaluation using multiple linear regression," *IEEE Sensors J.*, vol. 16, no. 5, pp. 1351–1360, Mar. 2016.
- [74] M. Borga and H. Knutsson, "A canonical correlation approach to blind source separation," Dept. Biomed. Eng., Linköping Univ., Linköping, Sweden, Tech. Rep. LiU-IMT-EX-0062, 2001.
- [75] C. Wiede, J. Richter, and G. Hirtz, "Signal fusion based on intensity and motion variations for remote heart rate determination," in *Proc. IEEE Int. Conf. Imag. Syst. Techn. (IST)*, Oct. 2016, pp. 526–531.
- [76] J. Cheng, X. Chen, L. Xu, and Z. J. Wang, "Illumination variation-resistant video-based heart rate measurement using joint blind source separation and ensemble empirical mode decomposition," *IEEE J. Biomed. Health Informat.*, vol. 21, no. 5, pp. 1422–1433, Sep. 2017.
- [77] X. He, R. A. Goubran, and X. P. Liu, "Wrist pulse measurement and analysis using Eulerian video magnification," in *Proc. IEEE-EMBS Int. Conf. Biomed. Health Informat. (BHI)*, Las Vegas, NV, USA, Feb. 2016, pp. 41–44.
- [78] A. Alnaji and J. Chahl, "Non-contact heart activity measurement system based on video imaging analysis," *Int. J. Pattern Recognit. Artif. Intell.*, vol. 31, no. 2, pp. 1–21, 2017.
- [79] W. Wang, S. Stuijk, and G. de Haan, "A novel algorithm for remote photoplethysmography: Spatial subspace rotation," *IEEE Trans. Biomed. Eng.*, vol. 63, no. 9, pp. 1974–1984, Sep. 2016.
- [80] W. Wang, A. den Brinker, S. Stuijk, and G. de Haan, "Algorithmic principles of remote PPG," *IEEE Trans. Biomed. Eng.*, vol. 64, no. 7, pp. 1479–1491, Jul. 2016.
- [81] A. Alnaji and J. Chahl, "Contactless cardiac activity detection based on head motion magnification," *Int. J. Image Graph.*, vol. 17, no. 01, p. 1750001, 2017.
- [82] J. M. Bland and D. G. Altman, "Statistical methods for assessing agreement between two methods of clinical measurement," *Int. J. Nursing Stud.*, vol. 47, no. 8, pp. 931–936, 2010.



ALI AL-NAJI received the bachelor's degree in medical instrumentation engineering techniques from the Electrical Engineering Technical College, Middle Technical University, Baghdad, Iraq, in 2005, and the M.S. degree from the Electrical and Electronic Engineering Department, Technology University, Baghdad, in 2008. He is currently pursuing the Ph.D. degree with the School of Engineering, Electrical and Information Engineering, University of South Australia. His research interests include biomedical engineering, computer vision systems, and microcontroller applications.



JAVAN CHAHL (M'11) received the Ph.D. degree from The Australian National University. He joined the Defence Science and Technology Group (DST Group) as a Research Scientist in 1999. In 2011, he joined RMIT University as a Founding Professor of unmanned aerial vehicles. In 2012, he became the Chair of sensor systems, a joint appointment between the DST Group and the University of South Australia. He is a member of the Institute of Engineers Australia.

He was an elected fellow of the Royal Aeronautical Society in 2014.